Oncology Research, Vol. 24, pp. 205–214
Printed in the USA.

0965-0407/16 $90.00 + .00
DOI: http://dx.doi.org/10.3727/096504016X14648701447896
E-ISSN 1555-3906
www.cognizantcommunication.com

Knockdown of Zinc Transporter ZIP5 by RNA Interference Inhibits Esophageal Cancer Growth In Vivo

Qian Li, Jing Jin, Jianghui Liu, Liqun Wang, and Yutong He

Cancer Institute, Fourth Hospital of Hebei Medical University, Shijiazhuang, Hebei, China

We recently found that SLC39A5 (ZIP5), a zinc transporter, is overexpressed in esophageal cancer. Downregulation of ZIP5 inhibited the proliferation, migration, and invasion of the esophageal cancer cell line KYSE170 in vitro. In this study, we found that downregulation of SLC39A5 (ZIP5) by interference resulted in a significant reduction in esophageal cancer tumor volume and weight in vivo. COX2 (cyclooxygenase 2) expression was decreased and E-cadherin expression was increased in the KYSE170K xenografts, which was caused by the downregulation of ZIP5. However, we did not find that the downregulation of ZIP5 caused a change in the relative expressions of cyclin D1, VEGF (vascular endothelial growth factor), MMP9 (matrix metalloprotein 9), and Bcl-2 (B-cell lymphoma/leukmia-2) mRNA or an alteration in the average level of zinc in the peripheral blood and xenografts in vivo. Collectively, these findings indicate that knocking down ZIP5 by small interfering RNA (siRNA) might be a novel treatment strategy for esophageal cancer with ZIP5 overexpression.

Key words: SLC39A5 (ZIP5); Esophageal cancer; COX2; E-cadherin; Xenograft; Zinc

INTRODUCTION

Cancer of the esophagus is the eighth most common cancer in the world and the sixth most common cause of death from cancer. In 2012, there were an estimated 456,000 new cases (3.2% of the total) with an estimated 400,000 deaths (4.9% of the total). Approximately 80% of the cases worldwide occur in less developed areas (1). China is a region of high incidence of esophageal carcinoma. Esophageal cancer is the fifth most common cancer in China, with 287,000 new cases, and the fourth leading cause of death from cancer, with 211,000 deaths according to the China National Cancer Center (2). The 5-year relative survival rate for esophageal cancer patients is 20.9% in China, primarily attributed to the fact that most patients are diagnosed initially with terminal-stage cancer (3). As a region of high incidence, the residents of Cixian have the highest incidence of, and mortality from, esophageal cancer in China (4). Some studies in regions of high incidence suggest that zinc (Zn) was a risk factor for esophageal cancer. In Linxian, some studies found that Zn levels in cases with esophageal squamous cell carcinoma (ESCC) are lower than those in control cases, in both serum (81 vs. 91 μg/dl) and esophageal tissue (81 vs. 97 μg/g) (5,6). Moreover, much evidence indicates that Zn deficiency promotes the effects of *N*-nitrosomethylbenzylamine (NMBA)/4-NQO, which acts as an esophageal carcinogen in rodents (7,8).

The ZIP transporter is one Zn transporter, and many studies have confirmed that the ZIP transporter is associated with cancer. The ZIP family includes four subfamilies that contain 14 members. A study found that ZIP1 deficiency was related to prostate cancer, and ZIP1 supplementation was used as a treatment for prostate cancer (9). Some studies found that the expression of ZIP2 and ZIP3 was higher in normal prostate tissue than that in prostate cancer tissue (10). Li et al. (11) thought ZIP4 was overexpressed in pancreatic cancer and silencing ZIP4 in pancreatic cancer cell lines could inhibit metastasis, tumor size in nude mice, and increase survival of mice with cancer. ZIP6 was highly expressed in breast cancer, related to the epithelial–mesenchymal transition (EMT), and ZIP6 overexpression was associated with the invasion and metastasis of breast cancer (12,13). Taylor et al. (14) found the abnormal expression of ZIP7 could promote the invasive growth of breast cancer by increasing the activation of growth factor receptor. As an androgen cell membrane receptor, ZIP9 contributed to the apoptosis of testosterone-induced prostate cancer and

Address correspondence to Professor Yutong He, Cancer Institute, Fourth Hospital of Hebei Medical University, Shijiazhuang, Hebei 050011, China. Tel: +86-0311-86095613; Fax: +86-0311-86095613; E-mail: hytong69@yahoo.com

breast cancer by Zn transporter function (15,16). Kang et al. (17) found that ZIP11 deficiency was associated with high-grade glioma and IDH1 mutation.

ZIP5 is one LIV-1 subfamily member and is similar to the ZIP4 protein in sequence. ZIP5 plays an important role in dietary Zn element absorption and in regulating organismal Zn status (18). A study found that mouse ZIP5 mRNA abundance did not change in response to Zn, but the translation of this mRNA was found to be Zn responsive (18). In addition, mouse ZIP5 played a novel role in polarized cells by carrying out serosal-to-mucosal Zn transport (19). Geiser et al. (20) found that mouse ZIP5 functioned in acinar cells to protect against Zn-leading acute pancreatitis and decreased the process of zymophagy.

We previously reported that ZIP5 was overexpressed in human esophageal cancer tissue, and downregulation of ZIP5 inhibited the proliferation, migration, and invasion of an esophageal cancer cell line KYSE170 in vitro. Furthermore, the percentage of cells in the G_0/G_1 phase in the KYSE170K cell line was higher than that in the KYSE170S cell line. ZIP5 knockdown decreased the expression of COX2 and increased the expression of E-cadherin in vitro (21). To study the effect of ZIP5 downregulation on esophageal cancer in vivo, we established an esophageal cancer nude mouse model.

MATERIALS AND METHODS

Cell Culture

The human esophageal cancer cell lines KYSE70, KYSE150, KYSE170, KYSE180, KYSE510, Eca109, Eca9706, and CaES17 were donated by the MD Anderson Cancer Center, USA. They were cultured in RPMI-1640 medium (Hyclone, Logan, UT, USA) with 10% heat-inactivated fetal bovine serum (FBS; PAN, Adenbach, Germany) at 37°C in a 5% CO_2 humidified incubator. HEK293T cells were cultured in Dulbecco's modified Eagle's medium (DMEM; Gibco, USA) with sodium pyruvate and 10% FBS.

Construction of Recombinant Lentivirus

Small interfering RNA (siRNA) of three potential target sequences were obtained from Ambion. siRNA sequences (sense: CCUGCUGAGCAGGAGCAGAACCAUUACCU and antisense: AGGUAAUGGUUCUGCUCCUGCUCA-GCAGG) were confirmed after screening. For lentivirus construction, a 29-bp fragment (5′-CCUGCUGAGCAGGAGCAGAACCAUUACCU-3′) within the ZIP5 cDNA was chosen as the target for shZIP5. A scramble fragment (5′-TGGATCCAAGGTCGGGCAGGAAGAG-3′) was used as a negative control. Hu6-shRNA with primers Hu6-for (*Bam*HI) and short hairpin RNA-rev (shRNA-rev) was hybridized and cloned into a TA vector. Correct insertion of Hu6-shRNA was confirmed using restriction mapping and direct DNA sequencing. For lentivirus plasmid PSD31-Hu6 construction, TA-shRNA and the plasmid PSD31 were digested using *Bam*HI and the generated cDNA was purified. The purified PSD31 was dephosphorylated. The plasmids PSD31-ZIP5-shRNA were obtained from *Escherichia coli* and transformed with the recombinant-containing, purified TA-shRNA and dephosphorylated PSD31.

The lentivirus packaging system containing the PSD31 plasmid and the specific shRNA were cotransfected into 293T cells using MegaTran1.0 (OriGene, Rockville, MD, USA) according to the manufacturer's instructions. After 48 h, the supernatant was harvested and filtered through a 0.45-mm filter.

Lentivirus Infection and Stable Transduction

For stable transduction, KYSE170 cells were cultured in six-well plates (4×10^5/well) and transfected with lentivirus with PSD31-ZIP5-shRNA or PSD31-scramble-shRNA. After 24 h, the medium with 0.6 μg/ml puromycin was replaced by the original medium until all cells died from parallel experiments. The living cells became the stable cell line, and the generated cell lines were named KYSE170K and KYSE170S.

Tumor Cell Inoculation

To research the effect of ZIP5 on the tumorigenesis of esophageal cancer cells, an esophageal cancer xenograft nude mouse model was successfully established. Sixteen nude mice 6 weeks old were divided into two groups, 170K and 170S, for cell inoculation (eight mice in each group). A total of 5×10^6 170K and 170S cells in 0.2 ml of phosphate-buffered saline (PBS) (Corning, Manassas, VA, USA) were subcutaneously injected into the right flank of the nude mice. The xenograft size in each group was measured at 5, 7, 9, 11, and 35 days after inoculation using a microcaliper, and the tumor volume was calculated according to the following formula: volume = 1/2 length × width^2.

Quantitative Real-Time PCR (qRT-PCR) Analysis

Total RNA was extracted with TRIquick reagent (Solarbio, Beijing, China) according to the operation manual. After the concentration and purity of the total RNA were determined by ultraviolet absorbance spectroscopy, RNA was reverse transcribed into cDNA using RevertAid First Strand cDNA Synthesis Kit (Thermo Scientific, Lithuania). qRT-PCRs using SuperReal PreMix Plus (SYBR Green) (TianGen, Beijing, China) were performed on ABI7500 Real-Time System (Life Technologies Corp., Foster City, CA, USA). The primers for ZIP5, COX2, E-cadherin, cyclin D1, VEGF (vascular endothelial growth factor), Bcl-2 (B-cell lymphoma/leukmia-2), MMP9 (matrix metalloprotein 9), and GAPDH (glyceraldehyde-3-phosphate

dehydrogenase) were designed and synthesized by Invitrogen (Carlsbad, CA, USA) (Table 1). The relative quantification was presented by the $2^{-\Delta\Delta Ct}$ method with normalization to GAPDH.

Western Blot Analysis

KYSE170K and KYSE170S were washed twice with ice-cold PBS and lysed with ice-cold lysis buffer (RIPA; BestBio, Shanghai, China), and xenografts (30 mg) were ground using an automatic muller with ice-cold lysis buffer in ice for 30 min at 4°C. Cell and tissue lysates were collected and centrifuged (14,000 rpm, 15 min, 4°C). The supernatants were collected, and the protein concentration was determined by BCA Protein Assay Kit (MultiSciences, Hanzhou, China). Total protein (50 μg) was separated with 10% SDS-polyacrylamide gel electrophoresis and then transferred to a polyvinylidene difluoride (PVDF) membrane. After the membranes were blocked with 5% nonfat milk for 1.5 h at room temperature, they were incubated with rabbit anti-ZIP5 polyclonal antibody (1:500) (Sigma-Aldrich, St. Louis, MO, USA) or anti-COX2 monoclonal antibody (1:800) (Cell Signaling, Danvers, MA, USA) or rabbit anti-E-cadherin polyclonal antibody (1:1,000) (Cell Signaling) or rabbit anti-GAPDH polyclonal antibody (Huabio, Hangzhou, China), which was used as a control (1:1,000) overnight at 4°C. The membranes were incubated with a secondary antibody for 1 h at room temperature in a dark room. The signals of objective proteins were detected on Odyssey infrared laser imaging system (LI-COR, Lincoln, NE, USA).

Immunohistochemical Staining

Xenografts were collected and cut into 5-μm paraffin slices. The slices were dewaxed and rehydrated, and then treated with 0.02 M EDTA buffer (pH 9.0; Gene Tech, Shanghai, China) in a super-pressure kettle for 7 min. To eliminate endogenous hydrogen peroxide enzyme activity, the slides were soaked in 3% H_2O_2 and blocked with normal goat serum (ZSGB-BIO, Beijing, China) for 45 min at 37°C, followed by incubation with rabbit anti-ZIP5 polyclonal antibody (1:200) (Sigma-Aldrich) or rabbit anti-COX2 monoclonal antibody (1:200) (Cell Signaling) or rabbit anti-E-cadherin polyclonal antibody (1:800) (Cell Signaling) overnight at 4°C. Then slices were incubated with the appropriate biotinylated secondary antibodies and streptavidin horseradish peroxidase (ZSGB-BIO) step by step for 30 min at 37°C. The sections were colored with 3,3′-diaminobenzidine tetrahydrochloride (DAB; ZSGB-BIO) and observed under a phase-contrast microscope.

Flow Cytometry (FCM) Assays

Xenografts were fixed in 70% cold ethanol (YongDa Chemical reagent, Tianjin, China) for 1 day at 4°C, and the cells were collected by rubbing. Propidium iodide (PI) fluorochrome solution was added into the cells, and the mixed samples were incubated in the dark at room temperature for 30 min. Cell cycle distribution and apoptosis were measured using FCM (Beckman Coulter, Brea, CA, USA).

Zn Measurement

Peripheral blood was collected from the retro-orbital venous plexus of each mouse after anesthesia when the mice were sacrificed. The Zn levels in the peripheral blood and xenografts were measured by DRC-e inductively coupled plasma mass spectrometer according to the manufacturer's instruction (PerkinElmer, Waltham, MA, USA).

Table 1. Sequences of Real-Time PCR Primers

Primer	Sequence	Annealing T_m	Size
GAPDH	F: CGCTGAGTACGTCGTGGAGTC R: GCTGATGATCTTGAGGCTGTTGTC		172 bp
E-cadherin	F: TGCCCAGAAAATGAAAAAGG R: GTGTATGTGGCAATGCGTTC	57ºC	200 bp
SLC39A5	F: CTCATGCTTGCCATAACC R: AATCCTATTGCTCCTACTGG	60ºC	151 bp
Cyclin D1	F: CTGTGCTGCGAAGTGGAAACCAT R: TTCATGGCCAGCGGGAAGACCTC	57ºC	233 bp
COX2	F: GGCGCTCAGCCATACAG R: CCGGGTACAATCGCACTTAT	62ºC	103bp
Bcl-2	F: TGCGGCCTCTGTTTGATTTC R: CGGTGCTTGGCAATTAGTGG	60ºC	426 bp
VEGF	F: GCTCGGTGCTGGAATTTGAT R: AAAAGTTTCAGTGCGACGCC	60ºC	543 bp
MMP9	F: TTTGAGTCCGGTGGACGATG R: GCTCCTCAAAGACCGAGTCC	62ºC	197 bp

Statistical Analysis

All statistical data were performed using GraphPad Prism 5.01 (GraphPad Software, San Diego, CA, USA). The data were analyzed by the Student's *t*-test between the control group and the treatment group and shown as mean ± standard deviation (SD). A value of two-sided $p < 0.05$ was considered statistically significant.

RESULTS

Specific and Effective Knockdown of ZIP5 in Esophageal Cancer by Lentivirus-Mediated RNAi

To successfully obtain the lentiviral vector PSD31-ZIP5-shRNA containing the target gene of ZIP5 knockdown, shRNA that could transcribe the effective siRNA was synthesized (Fig. 1A) and was successfully linked into the lentiviral vector PSD31. The synthetic plasmids PSD31-ZIP5-shRNA were confirmed to be correct using enzyme cleavage (Fig. 1B).

To successfully obtain the ZIP5 knockdown esophageal cancer cell lines from KYSE170, KYSE170K, and the control group KYSE170S, the esophageal cancer cell line KYSE170 was infected with virus packaged with lentivirus plasmids PSD31-ZIP5-shRNA and PSD31-scramble-shRNA. To determine the knockdown potency, RT-PCR and Western blots were performed to examine the transcription and translation levels of ZIP5. The mRNA and the protein levels of ZIP5 in the KYSE170K cell line were significantly reduced by 79.01% and 77.84% compared to the control group (Fig. 2A and B).

Effect of ZIP5 Knockdown on Tumor Growth in Nude Mice

To determine the effect of ZIP5 knockdown on esophageal cancer growth in vivo, a xenograft nude mouse model was established. The KYSE170K and KYSE170S cells (5×10^6 cells, respectively) were implanted subcutaneously in the right shoulder of nude mice. After 5 days, tumors successfully formed subcutaneously in all mice (Fig. 3A). The average xenograft weight of the test group (0.44 ± 0.11 g) was significantly reduced compared to that of the control group (0.70 ± 0.08 g) at the time of sacrifice

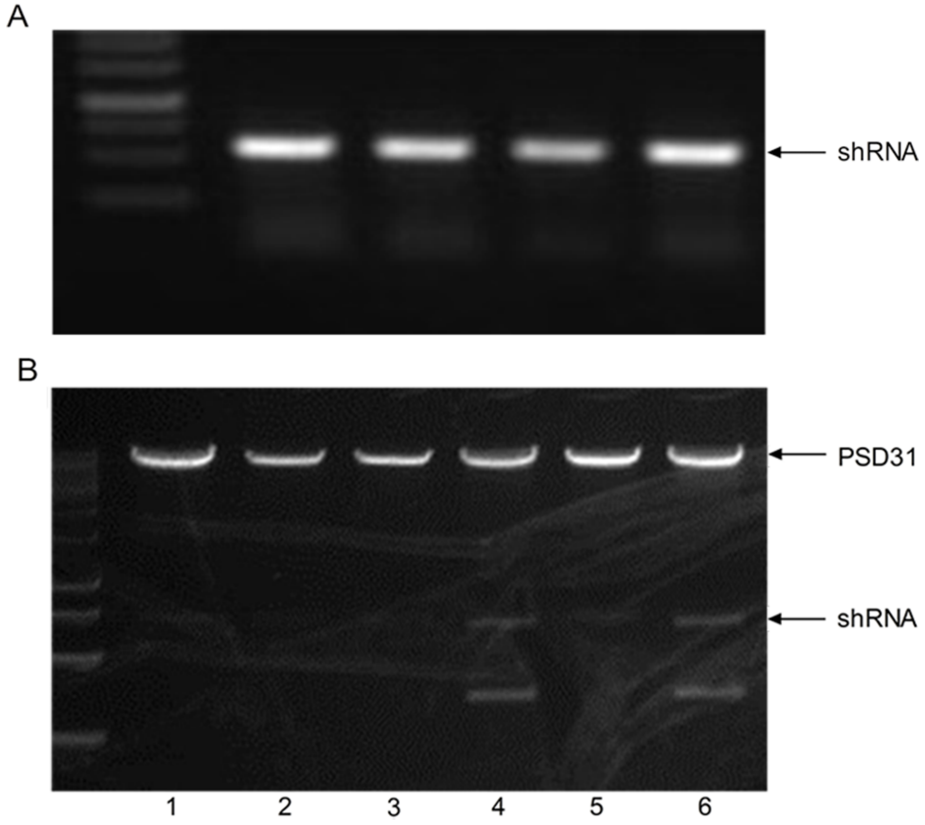

Figure 1. Lentivirus plasmid PSD31-ZIP5-shRNA. (A) The shRNA was confirmed by real-time polymerase chain reaction (RT-PCR). The shRNA transcribing the effective siRNA is located at 250 bp. (B) The synthetic plasmids PSD31-ZIP5-shRNA were confirmed correctly using enzyme cleavage. Lanes 1–6 are the DNA extracted from monoclonal *Escherichia coli* transformed with the recombinant-containing purified TA-shRNA and dephosphorylated PSD31. Lanes 4 and 6 are the plasmids synthesized successfully.

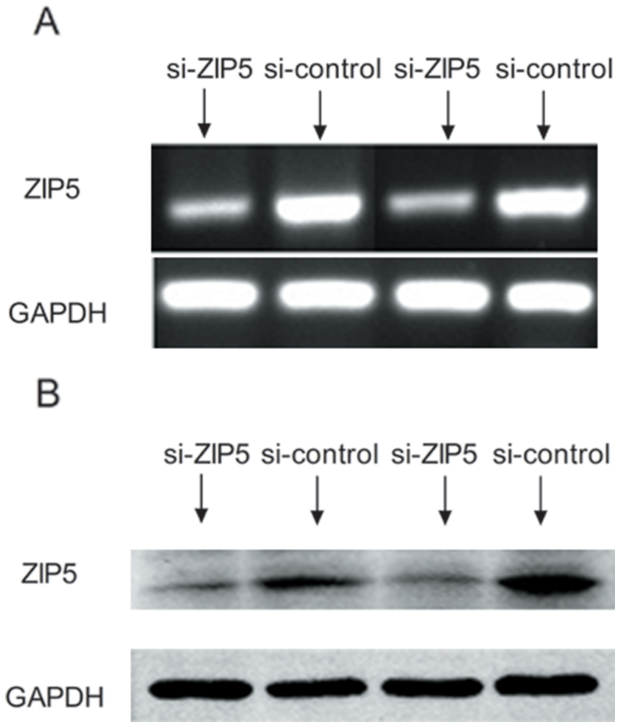

Figure 2. Lentivirus-mediated knockdown of ZIP5 in KYSE170 cells. (A) Expression of the ZIP5 mRNA was downregulated by lentivirus siRNA in KYSE170 cells by RT-PCR. (B) Expression of the ZIP5 protein was downregulated by lentivirus siRNA in KYSE170 cells by Western blot.

($p=0.007$) (Fig. 3B). The mean volume of tumors in the test group (614.50 ± 87.12 mm^3) was significantly smaller than that in the control group ($1{,}095.43\pm266.64$ mm^3) at the time of sacrifice ($p=0.012$) (Fig. 3C).

Molecular Expression Changes in the Esophageal Cancer Mouse Xenograft Model

To further probe molecular expression changes for ZIP5 knockdown in vivo, COX2, E-cadherin, cyclin D1, VEGF, MMP9, and Bcl-2 mRNA expression levels of the xenografts were detected using qRT-PCR. The relative level of ZIP5 mRNA in the test group was 0.46 ± 0.33, and 1.06 ± 0.43 in the control group. The relative level of ZIP5 mRNA in the test group was decreased by 57% in vivo (Fig. 4A). The relative level of COX2 mRNA in the test group was 0.64 ± 0.12, and 1.03 ± 0.25 in the control group. The relative level of COX2 mRNA in the test group was decreased by 38% in vivo, while the relative level of E-cadherin mRNA in the test group was 1.68 ± 0.31, and 1.00 ± 0.09 in the control group. The relative level of E-cadherin mRNA in the test group was increased by 68% in vivo. The relative levels of cyclin D1, VEGF, MMP9, and Bcl-2 mRNA in the test group were similar to the levels in the control group in vivo (all $p>0.05$).

The expression of the ZIP5 protein in the test group was 0.38 ± 0.02 and was 0.81 ± 0.13 in the control group. The expression of the ZIP5 protein in the test group was reduced by 53% in vivo (Fig. 4B). The expression of the COX2 protein in the test group was 0.13 ± 0.06 and was 0.33 ± 0.11 in the control group in vivo. The expression of the COX2 protein in test group was reduced by 61%. While the expression of the E-cadherin protein in the test group was 0.85 ± 0.05, it was 0.45 ± 0.04 in the control group. The expression of the E-cadherin protein in the test group was increased by 47% in vivo.

The ZIP5 protein score was 2.55 ± 0.34 in the test group and was 5.15 ± 1.74 in the control group. The COX2 protein score in the test group was 1.43 ± 0.69 and was 3.23 ± 1.29 in the control group. The E-cadherin protein score was 10.60 ± 1.33 and was 6.70 ± 1.64 in the control group in vivo by immunohistochemical staining (Fig. 4C).

The Effect of ZIP5 Knockdown on Zn Levels in the Peripheral Blood and Xenografts

To explore the effect of ZIP5 knockdown on the levels of Zn in the peripheral blood and xenografts, Zn concentrations were tested using a DRC-e inductively coupled plasma mass spectrometer. The average level of Zn in the peripheral blood of the test group was 2.47 ± 0.27 mg/kg, compared to 2.48 ± 0.28 mg/kg in the control group ($p>0.05$). The mean concentration of Zn in the xenograft test group was 20.30 ± 3.28 mg/kg, compared to 19.60 ± 3.85 mg/kg in the control group ($p>0.05$) (Table 2).

DISCUSSION

Esophageal cancer ranks as the eighth most common cancer and as the sixth most common cause of death from cancer in the world according to GLOBCAN 2012 (1). The Hebei province is a high-risk area for esophageal cancer in China. In particular, the incidence and mortality of esophageal cancer in Cixian are among the highest in the world (22). As a common malignancy, the esophageal cancer survival rate is very poor, and the 5-year relative survival rate for esophageal cancer patients is 20.9% in China (3). It is very important to study the mechanisms of the development of esophageal cancer.

Zn plays a crucial role in metabolism as an essential trace element with antioxidant properties (23). Zn acts as an intracellular signaling molecule, plays a role in communicating between cells by converting extracellular stimuli to intracellular signals, and controls intracellular events. Abnormal Zn homeostasis can lead to a variety of health problems including growth retardation, hypogonadism, immunodeficiency, and neuronal and sensory dysfunctions (24). Some studies suggested that Zn was a risk factor for ESCC. In these studies, Abnet et al. (25) indicated that dietary Zn deficiency had a strong association with

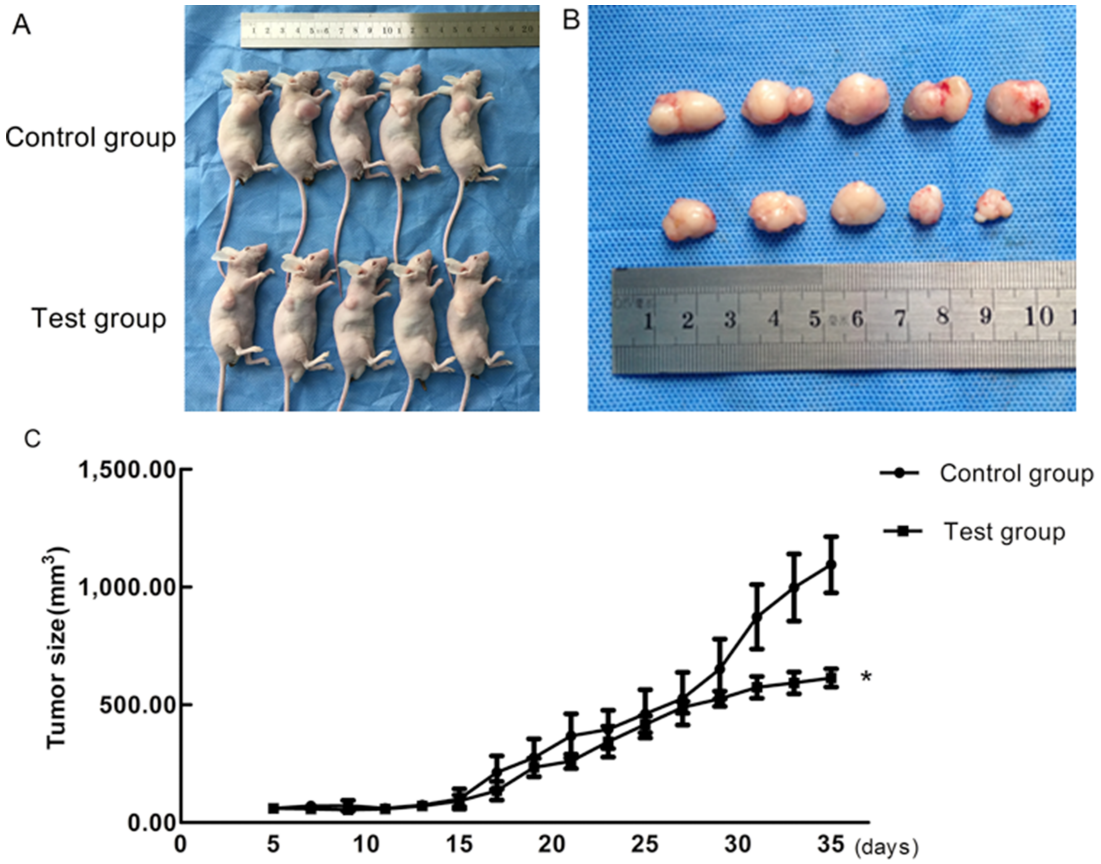

Figure 3. Lentivirus-mediated knockdown of ZIP5 inhibits tumor growth in nude mice. KYSE170K and KYSE170S cells were subcutaneously injected into the right shoulder of nude mice. (A) Five days after injection, the xenografts were formed, and then all mice were sacrificed and the xenografts were dissociated. (B) The images of xenografts are shown. (C) Tumor volume was calculated at 5, 7, 9, and 35 days after tumors formed using a microcaliper. The average xenograft volume of the test group was significantly inhibited compared to the control group ($*p<0.05$).

ESCC in the high-incidence region by finding an inverse relationship between Zn levels in biopsy samples and the subsequent risk of advancing to ESCC. Taccioli et al. (26) provided that long-term Zn deficiency alone caused the overexpression of many inflammation genes and prolonged Zn deficiency and low doses of NMBA triggered ESCC. A meta-analysis of the relationship between Zn intake and risk of digestive tract cancers suggested that Zn intake was not significantly related to esophageal cancer [pooled relative risk (RR)=0.72, 95% confidence interval (CI)=0.44–1.17], but subgroup analysis showed that Zn intake was markedly associated with esophageal cancer and gastric cancer risk in Asia (highest vs. lowest categories; pooled RR=0.43, 95% CI=0.21–0.86), but not in the US or Europe (27).

Zn homeostasis is regulated by the Zn transporter and permeable channels. Replenishing cytosolic Zn from the extracellular space and the lumens of intracellular compartments is the main function of ZIP transporters. ZIP transporters are localized to the plasma membrane, Golgi apparatus, endoplasmic reticulum, and endosomes/lysosomes (28). ZIP transporters have eight predicted transmembrane helices with extracellular/luminal NH_2 and COOH termini facing the extracytoplasmic space (29). It was reported that the ZIP family was associated with a variety of tumors, such as prostate cancer, pancreatic cancer, breast cancer, and esophageal cancer (30–33). ZIP1, ZIP2, and ZIP3 deficiencies were associated with prostate cancer (9,10). Makhov et al. (34) indicated that the core promoter region responsible for the expression of hZIP1 was SP1 and CREB in prostate cancer cells. Li et al. (11) indicated that the silencing of ZIP4 in ASPC-1 and BxPC-3 would decrease cell proliferation, migration, and invasion and inhibit tumor volume and weight in the nude mouse subcutaneous model. In another study, Zhang et al. (35) found that a novel mechanism of increased Zn mediated by ZIP4 transcriptionally induced miR-373 (ZIP4-CREB-miR-373 signaling channel) in pancreatic cancer promoted tumor growth. For prostate cancer, the expression of ZIP4 mRNA and protein was markedly

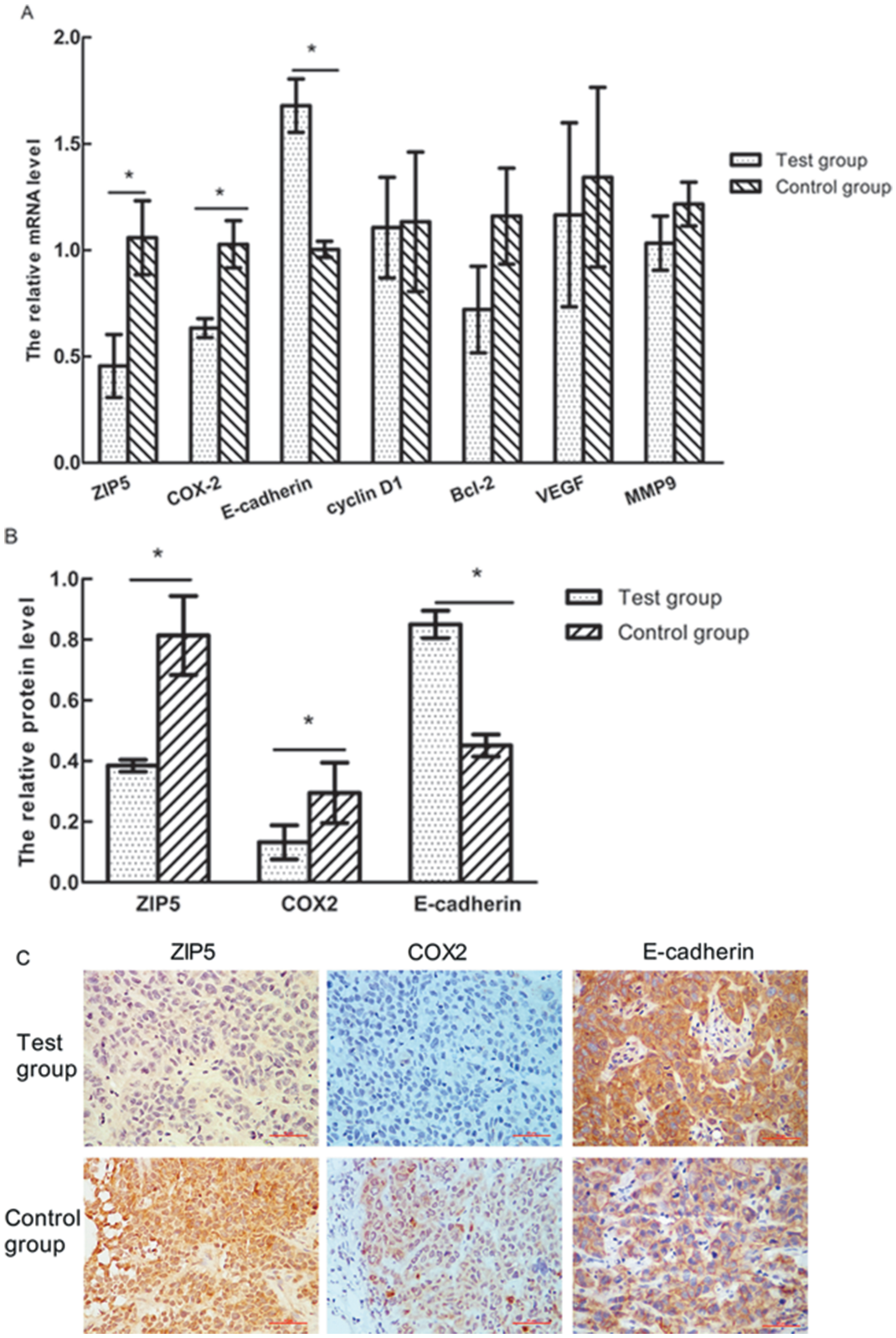

Figure 4. (A) Changes of molecular expression in esophageal cancer xenografts. Downregulation of ZIP5 could inhibit the mRNA expression level of COX2 and elevate the mRNA expression level of E-cadherin using qRT-PCR ($*p<0.05$). (B, C) Downregulation of ZIP5 could inhibit the protein expression of COX2 and elevate the protein expression level of E-cadherin using Western blot and immunohistochemistry (40×) ($*p<0.05$).

Table 2. The Zinc Levels of Peripheral Blood and Xenograft

Group	Mean ± SD (mg/kg)	*n*	*t*	*p*
Peripheral blood		16	−0.01	0.99
Test group	2.47 ± 0.27	8		
Control group	2.48 ± 0.28	8		
Xenograft		16	0.36	0.72
Test group	20.30 ± 3.28	8		
Control group	19.60 ± 3.85	8		

downregulated in tumor tissues compared with benign prostate hyperplasia tissues (36). Lin et al. (37) suggested that ZIP4 overexpression was significantly associated with a higher grade of gliomas and shorter overall survival in two independent cohorts. Many studies indicated that the dysregulated expression of ZIP6 was associated with cell invasion and metastasis in breast cancer. ZIP6 was transcriptionally induced by STAT3 and activated by N-terminal cleavage, which attracted ZIP6 to the plasma membrane; Zn influx inactivates GSK-3β (glycogen synthase kinase 3β), either indirectly or directly via Akt or GSK-3β, respectively. This results in the activation of Snail, which remains in the nucleus and acts as a transcriptional repressor of E-cadherin (epithelial cadherin), and CDH1, causing cell rounding and detachment in breast cancer (30). Wu et al. (31) showed that higher expression of the ZIP6 protein was correlated with a shorter length of survival in patients with advanced ESCC by immunohistochemical staining ($p = 0.013$). Taylor et al. (38) found that the removal of ZIP7 destroyed the activation of epithelial growth factor receptor/IGF receptor/Src signaling by reducing intracellular Zn levels, and increased tumor killing, preventing further development of resistance in breast cancer.

Wang et al. (19) found that except for ZIP5, ZIP transporters' cell surface location increases under Zn-deficient conditions. The biological function of ZIP5 is not well known. It was reported that mouse ZIP5 localized to the basolateral surfaces of enterocytes, acinar cells, and visceral endoderm cells when Zn was adequate. Interestingly, it was removed from those cell surfaces and internalized during Zn deficiency (39). Wang et al. (19) deemed that ZIP5 played a novel role in polarized cells by carrying out serosal-to-mucosal Zn transport. Weaver et al. (18) suggested that ZIP5 mRNA associated with polysomes, while the protein was internalized and degraded in enterocytes, acinar cells, and endoderm cells during Zn deficiency. ZIP5 was quickly resynthesized and targeted to the basolateral plasma membranes. Kumar et al. (40) found the upregulation of the Zn transporter ZIP5 and downregulation of the Zn metabolizing protein metallothionein MT1G in ESCC using a cDNA microarray and suggested deregulation of Zn homeostasis in esophageal tumorigenesis.

We previously reported that ZIP5 was overexpressed in human esophageal cancer tissue in regions of high incidence, and downregulation of ZIP5 inhibited the proliferation, migration, and invasion of esophageal cancer in vitro (21). To explore the effect of ZIP5 knockdown on esophageal cancer progression in vivo, a stably transducted esophageal cancer cell line of ZIP5 knockdown was successfully established in this study. Our results showed that the downregulation of ZIP5 remarkably inhibited the growth of tumor in vivo. We found the rate of tumor growth in the test group was significantly lower than that in the control group. The tumor in the test group remained slow growing. The role of ZIP5 knockdown in inhibiting tumor growth was that growth of xenografts was slowed to a certain extent. Further study showed that the level of Zn in the test group was similar to the control group. We suggested that ZIP5 knockdown did not alter the level of Zn in the peripheral blood of mice with xenografts. Maintaining intracellular Zn homeostasis is a long-term cumulative effect by ZIP5, and the factors affecting the level of Zn in blood included the content of Zn in feed and the capacity of intestinal absorption. In this study, all mice were normal and given normal SPF maintenance growth feed. Moreover, mouse daily activities were not affected after esophageal cancer cells were inoculated, which may be factors that contributed to the maintenance of Zn levels in peripheral blood. The level of Zn in xenografts of the test group was similar to that in the control group, and ZIP5 knockdown did not change the level of Zn in the xenografts. The reasons remain to be studied further. To study the impact of Zn, we will use different Zn content fodder to feed the mice with tumors.

We found that the mRNA and protein expression levels of COX2 were reduced by 38% and 61%, respectively, in vivo. While the mRNA and protein expression levels of E-cadherin were elevated by 68% and 47%, respectively, in vivo, the expression of cyclin D1 mRNA was not changed in vivo.

COX2 is a key enzyme in prostaglandin compounding and is one target gene of NF-κB (nuclear factor κB). COX2 is an important molecular basis for cancer progression. COX2 overexpression can promote the proliferation of tumors and the invasive ability of cancer and inhibit cancer cell apoptosis. Furthermore, it is associated with the prognosis of patients with tumors (41,42). Currently, the relationship between the expression of COX2 and the signaling pathway is not clear. Studies suggest that COX2 was overexpressed in ESCC, especially in a well-differentiated carcinoma, and the expression of COX2 was regulated by NF-κB (43). Fong et al. (44) found that COX2 overexpression accompanied hyperplasia in Zn deficiency, and Zn regulated COX2 expression in vivo. We previously reported that COX2 was overexpressed in esophageal cancer (21). These findings are

consistent with the idea that COX2 overexpression can facilitate tumor formation.

Chen et al. (45) suggested that COX2 activated NF-κB, thus regulating the transcription and expression of E-cadherin through the Snail signaling pathway in gastric cancer. E-cadherin located in epithelial cells is a calcium-dependent transmembrane protein, regulates the EMT, and participates in cell-to-cell adhesion. E-cadherin can inhibit the dedifferentiation and malignant proliferation of cancer cells and can inhibit cancer cell invasion and metastasis. A previous study suggested that E-cadherin deficiency was associated with cancer invasion, metastasis, and prognosis in a variety of tumors (46). In this study, we suggested that ZIP5 knockdown inhibited the growth of xenografts in vivo through decreased COX2 expression and elevated E-cadherin expression.

The percentage of cells in the G_0/G_1 phase and apoptosis were detected by FCM. The average percentage of cells in the G_0/G_1 phase in the test group was 48.94 ± 4.46% compared to 46.30 ± 2.78% in the control group. The average numbers of apoptosis cells in the test group and control group were 32.50 ± 5.24% and 37.16 ± 4.40%, respectively. There were no differences in the percentage of cells in the G_0/G_1 phase or in the apoptosis cells between the test and control groups. Furthermore, there were no differences in the relative expression of cyclin D1 mRNA between the test and control groups. Further studies are needed to determine the reasons we did not observe any differences.

In summary, we found that downregulation of ZIP5 by RNA interference inhibited esophageal cancer growth in vivo, reduced the expression of COX2, and promoted the expression of E-cadherin. These results suggest that the downregulation of ZIP5 will be a therapy for esophageal cancer.

ACKNOWLEDGMENT: This study was supported by grants from the National Natural Scientific Foundation of China (No. 81272682).

REFERENCES

1. International Agency for Research on Cancer. Oesophageal cancer: Estimated incidence, mortality and prevalence worldwide 2012. Retrieved from http://globocan.iarc.fr/Pages/fact_sheets_cancer.aspx?cancer=oesophagus
2. Chen, W. Q.; Zheng, R. S.; Zuo, T. T.; Zeng, H. M.; Zhang, S. W.; He, M. National cancer incidence and mortality in China, 2012. Chin. J. Cancer Res. 28:1–11; 2016.
3. Zeng, H.; Zheng, R.; Guo, Y.; Zhang, S.; Zou, X.; Wang, N.; Zhang, L.; Tang, J.; Chen, J.; Wei, K.; Huang, S.; Wang, J.; Yu, L.; Zhao, D.; Song, G.; Chen, J.; Shen, Y.; Yang, X.; Gu, X.; Jin, F.; Li, Q.; Li, Y.; Ge, H.; Zhu, F.; Dong, J.; Guo, G.; Wu, M.; Du, L.; Sun, X.; He, Y.; Coleman, M. P.; Baade, P.; Chen, W.; Yu, X. Q. Cancer survival in China, 2003–2005: A population-based study. Int. J. Cancer 136:1921–1930; 2015.
4. He, Y. T.; Wu, Y.; Song, G.; Li, Y.; Liang, D.; Jin, J.; Wen, D.; Shan, B. Incidence and mortality rate of esophageal cancer has decreased during past 40 years in Hebei Province, China. Chin. J. Cancer Res. 27:562–571; 2015.
5. Zheng, S. F.; Liu, X. F.; Li, Q. L. The preliminary analysis of serum concentration of copper, iron, magnesium and zinc in esophageal cancer patients and normal controls. Cancer Res. Prev. Treat. (Chinese) 8:4–7; 1980.
6. Hu, G. G.; Luo, X. M.; Shang, A. L.; Qin, Q. S. Trace elements in esophageal cancer—Analysis of 44 cases. Zhongguo Yi Xue Ke Xue Yuan Xue Bao 4:178–180; 1982.
7. Fong, L. Y.; Farber, J. L.; Magee, P. N. Zinc replenishment reduces esophageal cell proliferation and N-nitrosomethylbenzylamine (NMBA)-induced esophageal tumor incidence in zinc-deficient rats. Carcinogenesis 19:1591–1596; 1998.
8. Fong, L. Y.; Nguyen, V. T.; Farber, J. L. Esophageal cancer prevention in zinc-deficient rats: Rapid induction of apoptosis by replenishing zinc. J. Natl. Cancer Inst. 93:1525–1533; 2001.
9. Costello, L. C.; Franklin, R. B.; Zou, J.; Naslund, M. J. Evidence that human prostate cancer is a ZIP1-deficient malignancy that could be effectively treated with a zinc ionophore (clioquinol) approach. Chemotherapy (Los Angel). 4:152; 2014.
10. Desouki, M. M.; Geradts, J.; Milon, B.; Franklin, R. B.; Costello, L. C. hZip2 and hZip3 zinc transporters are down regulated in human prostate adenocarcinomatous glands. Mol. Cancer 6:37; 2007.
11. Li, M.; Zhang, Y.; Bharadwaj, U.; Zhai, Q. J.; Ahern, C. H.; Fisher, W. E.; Brunicardi, F. C.; Logsdon, C. D.; Chen, C.; Yao, Q. Down-regulation of ZIP4 by RNA interference inhibits pancreatic cancer growth and increases the survival of nude mice with pancreatic cancer xenografts. Clin. Cancer Res. 15:5993–6001; 2009.
12. Shen, R.; Xie, F.; Shen, H.; Liu, Q.; Zheng, T.; Kou, X.; Wang, D.; Yang, J. Negative correlation of LIV-1 and E-cadherin expression in hepatocellular carcinoma cells. PLoS One 8:e56542; 2013.
13. Zhao, L.; Chen, W.; Taylor, K. M.; Cai, B.; Li, X. LIV-1 suppression inhibits HeLa cell invasion by targeting ERK1/2-Snail/Slug pathway. Biochem. Biophys. Res. Commun. 363:82–88; 2007.
14. Taylor, K. M.; Hiscox, S.; Nicholson, R. I.; Hogstrand, C.; Kille, P. Protein kinase CK2 triggers cytosolic zinc signaling pathways by phosphorylation of zinc channel ZIP7. Sci. Signal. 5:ra11; 2012.
15. Thomas, P.; Pang, Y.; Dong, J.; Berg, A. H. Identification and characterization of membrane androgen receptors in the ZIP9 zinc transporter subfamily: II. Role of human ZIP9 in testosterone-induced prostate and breast cancer cell apoptosis. Endocrinology 155:4250–4265; 2014.
16. Berg, A. H.; Rice, C. D.; Rahman, M. S.; Dong, J.; Thomas, P. Identification and characterization of membrane androgen receptors in the ZIP9 zinc transporter subfamily: I. Discovery in female Atlantic croaker and evidence ZIP9 mediates testosterone-induced apoptosis of ovarian follicle cells. Endocrinology 155:4237–4249; 2014.
17. Kang, X.; Chen, R.; Zhang, J.; Li, G.; Dai, P. G.; Chen, C.; Wang, H. J. Expression profile analysis of zinc transporters (ZIP4, ZIP9, ZIP11, ZnT9) in gliomas and their correlation with IDH1 mutation status. Asian Pac. J. Cancer Prev. 16:3355–3360; 2015.
18. Weaver, B. P.; Dufner-Beattie, J.; Kambe, T.; Andrews, G. K. Novel zinc-responsive post-transcriptional mechanisms reciprocally regulate expression of the mouse Slc39a4 and

Slc39a5 zinc transporters (Zip4 and Zip5). Biol. Chem. 388:1301–1312; 2007.
19. Wang, F.; Kim, B. E.; Petris, M. J.; Eide, D. J. The mammalian Zip5 protein is a zinc transporter that localizes to the basolateral surface of polarized cells. J. Biol. Chem. 279:51433–51441; 2004.
20. Geiser, J.; De, Lisle, R. C.; Andrews, G. K. The zinc transporter Zip5 (Slc39a5) regulates intestinal zinc excretion and protects the pancreas against zinc toxicity. PLoS One 8:e82149; 2013.
21. Jin, J.; Li, Z. X.; Liu, J. H.; Wu, Y.; Gao, X.; He, Y. T. Knockdown of zinc transporter ZIP5 (SLC39A5) expression significantly inhibits human esophageal cancer progression. Oncol. Rep. 34:1431–1439; 2015.
22. He, Y. T.; Hou, J.; Chen, Z. F.; Qiao, C. Y.; Song, G. H.; Meng, F. S.; Jin, H. X.; Chen, C. Trends in incidence of esophageal and gastric cardia cancer in high-risk areas in China. Eur. J. Cancer Prev. 17:71–76; 2008.
23. Hao, Q.; Maret, W. Imbalance between pro-oxidant and pro-antioxidant functions of zinc in disease. J. Alzheimer's Dis. 8:161–170; 2005.
24. Fukada, T.; Yamasaki, S.; Nishida, K.; Murakami, M.; Hirano, T. Zinc homeostasis and signaling in health and diseases. J. Biol. Inorg. Chem. 16:1123–1134; 2011.
25. Abnet, C. C.; Lai, B.; Qiao, Y. L.; Vogt, S.; Luo, X. M.; Taylor, P. R.; Dong, Z. W.; Mark, S. D.; Dawsey, S. M. Zinc Concentration in esophageal biopsy specimens measured by X-ray fluorescence and esophageal cancer risk. J. Natl. Cancer Inst. 97:301–306; 2005.
26. Taccioli, C.; Chen, H.; Jiang, Y.; Liu, X. P.; Huang, K.; Smalley, K. J.; Farber, J. L.; Croce, C. M.; Fong, L. Y. Dietary zinc deficiency fuels esophageal cancer development by inducing a distinct inflammatory signature. Oncogene 31:4550–4558; 2012.
27. Li, P.; Xu, J.; Shi, Y.; Chen, K.; Yang, J.; Wu, Y. Association between zinc intake and risk of digestive tract cancers: A systematic review and meta-analysis. Clin. Nutr. 33:415–420; 2014.
28. Kambe, T.; Tsuji, T.; Hashimoto, A.; Itsumura, N. The physiological, biochemical, and molecular roles of zinc transporters in zinc homeostasis and metabolism. Physiol. Rev. 95:749–784; 2015.
29. Jeong, J.; Eide, D. J. The SLC39 family of zinc transporters. Mol. Aspects Med. 34:612–619; 2013.
30. Hogstrand, C.; Kille, P.; Ackland, M. L.; Hiscox, S.; Taylor, K. M. A mechanism for epithelial-mesenchymal transition and anoikis resistance in breast cancer triggered by zinc channel ZIP6 and STAT3 (signal transducer and activator of transcription 3). Biochem. J. 455:229–237; 2013.
31. Wu, C.; Li, D.; Jia, W.; Hu, Z.; Zhou, Y.; Yu, D.; Tong, T.; Wang, M.; Lin, D.; Qiao, Y.; Zhou, Y.; Chang, J.; Zhai, K.; Wang, M.; Wei, L.; Tan, W.; Shen, H.; Zeng, Y.; Lin, D. Genome-wide association study identifies common variants in SLC39A6 associated with length of survival in esophageal squamous-cell carcinoma. Nat. Genet. 45:632–638; 2013.
32. Zhang, Q.; Sun, X.; Yang, J.; Ding, H.; LeBrun, D.; Ding, K.; Houchen, C. W.; Postier, R. G.; Ambrose, C. G.; Li, Z.; Bi, X.; Li, M. ZIP4 silencing improves bone loss in pancreatic cancer. Oncotarget 6:26041–26051; 2015.
33. Franklin, R. B.; Ma, J.; Zou, J.; Guan, Z.; Kukoyi, B. I.; Feng, P.; Costello, L. C. Human ZIP1 is a major zinc uptake transporter for the accumulation of zinc in prostate cells. J. Inorg. Biochem. 96:435–442; 2003.
34. Makhov, P.; Golovine, K.; Uzzo, R. G.; Wuestefeld, T.; Scoll, B. J.; Kolenko, V. M. Transcriptional regulation of the major zinc uptake protein hZip1 in prostate cancer cells. Gene 431:39–46; 2009.
35. Zhang, Y.; Yang, J.; Cui, X.; Chen, Y.; Zhu, V. F.; Hagan, J. P.; Wang, H.; Yu, X.; Hodges, S. E.; Fang, J.; Chiao, P. J.; Logsdon, C. D.; Fisher, W. E.; Brunicardi, F. C.; Chen, C.; Yao, Q.; Fernandez-Zapico, M. E.; Li, M. A novel epigenetic CREB-mR-373 axis mediates ZIP4-induced pancreatic cancer growth. EMBO Mol. Med. 5:1322–1334; 2013.
36. Chen, Q. G.; Zhang, Z.; Yang, Q; Shan, G. Y.; Yu, X. Y.; Kong, C. Z. The role of zinc transporter ZIP4 in prostate carcinoma. Urol. Oncol. 30:906–911; 2012.
37. Lin, Y.; Chen, Y.; Wang, Y.; Yang, J.; Zhu, V. F.; Liu, Y.; Cui, X.; Chen, L.; Yan, W.; Jiang, T.; Hergenroeder, G. W.; Fletcher, S. A.; Levine, J. M.; Kim, D. H.; Tandon, N.; Zhu, J. J.; Li, M. ZIP4 is a novel molecular marker for glioma. Neuro. Oncol. 15:1008–1016; 2013.
38. Taylor, K. M.; Vichova, P.; Jordan, N.; Hiscox, S.; Hendley, R.; Nicholson, R. I. ZIP7-mediated intracellular zinc transport contributes to aberrant growth factor signaling in antihormone-resistant breast cancer cells. Endocrinology 149:4912–4920; 2008.
39. Dufner-Beattie, J.; Kuo, Y. M.; Gitschier, J.; Andrews, G. K. The adaptive response to dietary zinc in mice involves the differential cellular localization and zinc regulation of the zinc transporters ZIP4 and ZIP5. J. Biol. Chem. 279:49082–49090; 2004.
40. Kumar, A.; Chatopadhyay, T.; Raziuddin, M.; Ralhan, R. Discovery of deregulation of zinc homeostasis and its associated genes in esophageal squamous cell carcinoma using cDNA microarray. Int. J. Cancer 120:230–242; 2007.
41. Yang, Z.; Guan, B.; Men, T.; Fujimoto, J.; Xu, X. Comparable molecular alterations in 4-nitroquinoline 1-oxide-induced oral and esophageal cancer in mice and in human esophageal cancer, associated with poor prognosis of patients. In Vivo 27:473–484; 2013.
42. Huang, J. X.; Xiao, W.; Chen, W. C.; Lin, M. S.; Song, Z. X.; Chen, P.; Zhang, Y. L.; Li, F. Y.; Qian, R. Y.; Salminen, E. Relationship between COX-2 and cell cycle-regulatory proteins in patients with esophageal squamous cell carcinoma. World J. Gastroenterol. 16:5975–5981; 2010.
43. Yang, G. Z.; Li, L.; Ding, H. Y.; Zhou, J. S. Cyclooxygenase-2 is over-expressed in Chinese esophageal squamous cell carcinoma, and correlated with NF-kappaB: An immunohistochemical study. Exp. Mol. Pathol. 79:214–218; 2005.
44. Fong, L. Y.; Zhang, L.; Jiang, Y.; Farber, J. L. Dietary zinc modulation of COX-2 expression and lingual and esophageal carcinogenesis in rats. J. Natl. Cancer Inst. 97:40–50; 2005.
45. Chen, Z.; Liu, M.; Liu, X.; Huang, S.; Li, L.; Song, B.; Li, H.; Ren, Q.; Hu, Z.; Zhou, Y.; Qiao, L. COX-2 regulates E-cadherin expression through the NF-kappaB/Snail signaling pathway in gastric cancer. Int. J. Mol. Med. 32:93–100; 2013.
46. Li, K.; He, W.; Lin, N.; Wang, X.; Fan, Q. X. N-cadherin knockdown decreases invasiveness of esophageal squamous cell carcinoma in vitro. World J. Gastroenterol. 15: 697–704; 2009.